Models for Terminal Ni(S-Cysteine) Modification in [NiFe]Hydrogenases by Iodoacetamide and Iodoacetate

Jason J. Smee,[a] Dawn C. Goodman,[a] Joseph H. Reibenspies,[a] and Marcetta Y. Darensbourg*[a]

Keywords: Nickel / Sulfur ligands / Hydrogenases / Bioinorganic chemistry

The *cis*-dithiolate complex [*N*,*N*′-bis(2-mercaptoethyl-2-methylpropyl)-1,5-diazacyclooctane]nickel(II) (**Ni-1***) **reacts with stoichiometric amounts of iodoacetamide to yield *S*-alkylated, mono- and diacetamide complexes, [(AA)Ni-1*][I] and [$(AA)_2$Ni-1*][$I]_2$. Their molecular structures are established by X-ray crystallography and find the former in pseudo-square planar geometry with no additional coordination of the amide functionality, while the latter is an octahedral $N_2S_2O_2Ni^{II}$ complex. The assignment of the axial coordination ligands as amide oxygen atoms is consistent with IR-spectroscopic ν(C=O) results both in the solid and solution states. The complexes are further characterized by UV/Vis spectroscopy, conductance measurements, and electrochemical studies. Comparisons are drawn between the alkylation of these simple dithiolate complexes and the loss of [NiFe]hydrogenase activity upon addition of alkylating agents.**

Introduction

Cysteine modification reagents such as sodium iodoacetate ($ICH_2CO_2^-Na^+$) and iodoacetamide [$ICH_2C(=O)NH_2$] are widely used to probe the involvement of cysteine residues in enzymatic systems.[1] S_N2 attack by the nucleophilic cysteinate sulfur atom produces *S*-(carboxymethyl)cysteine and *S*-(amidomethyl)cysteine, respectively (Scheme 1), which typically results in loss of catalytic activity. While Scheme 1 represents the reactive S as sulfhydryl, it is well known that deprotonated cysteines are more reactive towards alkylating agents. In some cases, the modified cysteine unit has been tracked by radiolabelling, thus permitting identification of the active site position in the protein. For example, the zinc metalloenzyme cobalamin-independent methionine synthase (MetE) contains a reactive zinc cysteinate residue at position 726 that is required for enzymatic activity.[2]

Iodoacetamide and acetylene were shown to inhibit the catalysis of H/D exchange of H_2/D_2O by the [NiFe]hydrogenase enzyme of *Thiocapsa roseopersicina*, the former irreversibly.[3] Inhibition by acetylene is reversible; upon removal of the acetylene, nearly maximal activity is restored. On placing the enzyme under acetylene and subsequently treating it with iodoacetamide, the H/D exchange was inhibited, but the activity could be partially restored by removing both the iodoacetamide and the acetylene. Notably, the irreversible inhibition by iodoacetamide occurs only in the reduced, active form of the enzyme. Alkylation with iodoacetamide in the oxidized, inactive form followed by reductive activation of the enzyme showed maximal H/D exchange activity. Although the alkylated residues were not identified, experiments which monitored the levels of ^{14}C-labeled *S*-(amidomethyl)cysteine indicated that the reduced enzyme contained a greater amount of cysteine modification in the portion of the protein containing the active site. These results suggest the possibility of active site modification.[3]

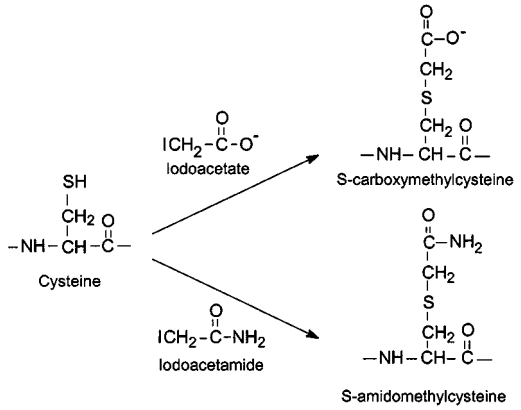

Scheme 1. Products resulting from alkylation of the cysteine sulfhydryl groups with iodoacetate and iodoacetamide; the other product, HI, is not shown

The X-ray crystal structure of an analogous [NiFe]H_2ase, isolated from *Desulfovibrio gigas* was recently solved[4a] and contains an $Ni(S-Cys)_4$ unit comprised of two terminal cysteines and two cysteines which bridge to an $Fe(CN)_2(CO)$ unit.[4b,4c] The oxidized state also contains a bridging ligand tentatively assigned as an oxo or hydroxo species, which is expected to be absent in the reduced or active form of the enzyme.[4b] Analysis of the X-ray crystal structure of *D. gigas* also reveals that the active site is buried ca. 30 Å from the protein surface with several cavities that converge on a unique entrance to the active site.[4b] In a separate study, xenon pressurization of crystals derived from *Desulfovibrio fructosovorans*, a [NiFe]H_2ase with sig-

[a] Department of Chemistry, Texas A&M University, College Station, TX 77843-3255, USA
Fax: (internat.) + 1-409/845-0158
E-mail: marcetta@mail.chem.tamu.edu

  1434–1948/99/0303–0539 $ 17.50+.50/0

nificant homology to *D. gigas*, confirmed the cavities to be a gas access channel.[5] It is thus tempting to conclude that the channel provides a means for H_2 molecules, as well as acetylene or iodoacetamide, to reach the active site. Experimentally, i.e., by the location of the Xe atoms, this channel was found to approach the active site at the terminal Ni(S−Cys) ligands, specifically $Ni-S-Cys_{530}$, to within 4 to 5 Å (Scheme 2). Electron density maps suggest that there are protein residues or water molecules which prevent closer contact. Molecular dynamics calculations find that H_2 molecules can, however, penetrate to within 1.4 and 1.8 Å of the nickel and iron atoms, respectively.[5] Since EPR and IR spectroscopies of [NiFe]H_2ases derived from various bacteria[4b,6,7] are similar to one another, it is reasonable to expect a similar active site composition, although gas access routes to the active site could differ.

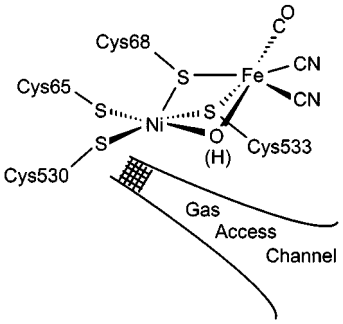

Scheme 2. A representation of the hydrophobic channel leading to the active site of *D. fructosovorans* [NiFe]H_2ase

Thus, the structural studies on [NiFe]H_2ases suggest some, and at most, limited, access to the active-site metal-bound cysteine. Indeed the specific residues alkylated by iodoacetamide in *T. roseopersicina* [NiFe]H_2ase have not been identified. Nevertheless there are examples of metal-bound cysteine modification at the active sites of other metalloproteins such as the zinc-containing MetE protein described above.[2] A fundamental question to be addressed by small molecule biomimics is, assuming active site access, will nickel-bound cysteines be alkylated by iodoacetamide or iodoacetate, and, if so, what are the structural, spectroscopic and electrochemical consequences?

One appropriate study, designed for other purposes, used the N_2S_2Ni square planar complex, *N*,*N*′-bis(mercaptoethyl)-1,5-diazacyclooctanenickel(II) (**Ni-1**).[8] The *cis*-dithiolate sulfur atoms of **Ni-1** are highly reactive with alkylating reagents, and in the case of sodium haloacetate salts, the **Ni-1** species yielded the octahedral $N_2S_2O_2$ complex shown in Equation 1.[8]

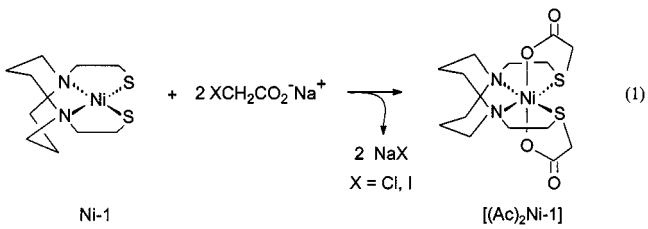

Given the relevance of these results to the [NiFe]H_2ase cysteine modification described above, we have explored similar reactions of **Ni-1** as well as the sterically more hindered *N*,*N*′-bis(2-mercapto-2-methylpropane)-1,5-diazacyclooctanenickel(II) (**Ni-1***) with iodoacetamide. Described below are the fully characterized products of **Ni-1*** reactions with one and two equivalents of iodoacetamide. The X-ray crystal structures will show the two possibilities of S-modification, i.e., with and without additional coordination of functional groups.

Results and Discussion

Syntheses and Solution Properties

In contrast to the reactions[8] of $XCH_2CO_2^-Na^+$ (X = Cl, I) with the parent (bme-daco)Ni (**Ni-1**) complex for which a monoalkylated complex could not be isolated (Equation 1), both the mono- and dialkylated species of **Ni-1** and the sterically encumbered **Ni-1*** have been isolated using iodoacetamide as the alkylating agent. Scheme 3 summarizes the synthetic procedures and stick-drawn structures resulting from structural characterization in the solid state (vida infra).

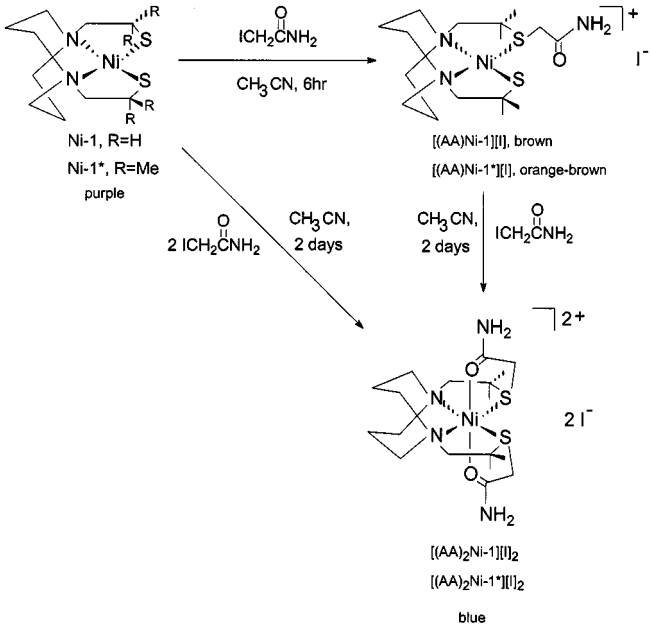

Scheme 3. Reactions of **Ni-1** and **Ni-1*** with one and two equivalents of iodoacetamide

As depicted in Scheme 3, the monoacetamide derivative of **Ni-1***, **[(AA)Ni-1*][I]**, is a four-coordinate pseudo-square planar complex and is soluble in most polar solvents including H_2O, MeOH and MeCN, all of which result in green solutions. In contrast, the brown solid **[(AA)Ni-1][I]** yields brown solutions in the same solvents. Minor differences in color are also seen for the **[(Me)Ni-1*][I]**[9] and **[(Me)Ni-1][I]**[10] species and are reflected in the d-d transitions as seen in Table 1 (see entries 3, 5, 7 and 9). The molar conductivities of **[(AA)Ni-1*][I]** and **[(AA)Ni-1][I]**,

measured in MeCN, are 166 and 161 S/cm·mol respectively, extrapolated to infinite dilution; these values fall in the range of uni-uni electrolyte solutions in CH_3CN[13] and indicate complete ionization of iodide in solution. Thus, we conclude that both **[(AA)Ni-1*][I]** and **[(AA)Ni-1][I]** are four-coordinate monocations in solution and the difference in color results from differences in ligand fields (see below).

The dialkylated products **[$(AA)_2$Ni-1*][I_2]** and **[$(AA)_2$Ni-1][I_2]** were isolated as blue solids with UV/Vis-spectral properties similar to those of **[$(Ac)_2$Ni-1]** (see entries 4, 6 and 11 of Table 1). For comparison, the dimethylated, four-coordinate derivatives **[$(Me)_2$Ni-1*][I_2]** and **[$(Me)_2$Ni-1][I_2]** have significantly different UV/Vis properties (entries 8 and 10 in Table 1) consistent with the conclusion that **[$(AA)_2$Ni-1*][I_2]** and **[$(AA)_2$Ni-1][I_2]** are six-coordinate complexes with Ni^{2+} in an $N_2S_2O_2$ coordination environment. **[$(AA)_2$Ni-1*][I_2]** and **[$(AA)_2$Ni-1][I_2]** are only slightly soluble in MeCN and are quite soluble in H_2O and MeOH, all of which yield blue solutions.

Table 1. UV/Vis[a] and IR[b] spectroscopic data (AA = *S*-acetamide; Ac = *S*-acetate; sh = shoulder)

Entry	Compound	λ_{max} [nm] (ε)	ν(C=O) [cm^{-1}]
1	Ni-1*[c,d]	353 sh, 498 (91)	–
2	Ni-1[c,e]	506 (640), 602 sh	–
3	[(AA)Ni-1*][I]	604 (51), 456 (124)	1684 (1692)
4	$[(AA)_2$Ni-1*][$I]_2$	580 (23), 356 (29)	1646s, 1591m[f] (1663s)
5	[(AA)Ni-1][I]	592 sh, 472 (137)	1676 (1713)
6	$[(AA)_2$Ni-1][$I]_2$	580 (36), 362 (51)	1649s, 1590m[f] (1663s)
7	[(Me)Ni-1*][I][c]	606 sh, 458 (150)	–
8	$[(Me)_2$Ni-1*][$I]_2$[c,g]	466 (115)	–
9	[(Me)Ni-1][I][c,e]	616 sh, 460 (130)	–
10	$[(Me)_2$Ni-1][$I]_2$[c,e]	656 (90), 428 (930)	–
11	$[(Ac)_2$Ni-1][h]	600 (49), 364 (31)	1593s, 1385m[d,f]
12	$CH_3C(=O)NH_2$	–	1690

[a] Data obtained in CH_3OH unless otherwise noted. – [b] IR data collected as KBr pellets, and, in parentheses, acetonitrile solution. – [c] Data obtained in CH_3CN. – [d] Ref.[11] – [e] Ref.[10] – [f] Assigned as an asymmetric carbonyl stretch. – [g] Ref.[12] – [h] Ref.[8]

Infrared Spectroscopy

Table 1 also lists the ν(C=O) stretching frequencies for acetamide, $CH_3C(=O)NH_2$, and for the complexes derivatized with iodoacetamide. The monoacetamide derivatives exhibit ν(C=O) values similar to free acetamide (entries 3, 5 and 12 in Table 1) whereas the diacetamide derivatives (entries 4 and 6 in Table 1) show a decrease of ca. 35 cm^{-1} in ν(C=O) relative to the monoacetamide complexes. This is consistent with the UV/Vis-spectroscopic results which suggest that oxygen binds to the nickel only in the case of the dialkylates **[$(AA)_2$Ni-1][I_2]** and **[$(AA)_2$Ni-1*][I_2]**. Thus, ν(C=O) is diagnostic for amide oxygen coordination to a metal center. Such shifts in the carbonyl stretching frequencies have been observed for other complexes with ligating amido groups.[14]

Electrochemistry

The cyclic voltammogram of **[(AA)Ni-1*][I]**, Figure 1, shows an irreversible cathodic event at $E_{pc} = -1.30$ V (vs NHE) and two oxidations ascribed to iodide electrochemistry. Figure 2, the cyclic voltammogram of **[$(AA)_2$Ni-1*][I_2]**, shows a quasi-reversible cathodic event at $E_{1/2} = -0.89$ V as well as a quasi-reversible anodic event at $E_{1/2} = +1.44$ V; two oxidations and one reduction due to iodide (or I_3^-) are also present.

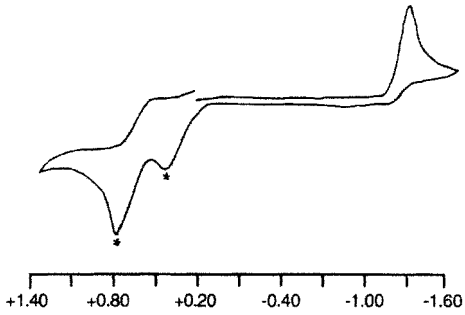

Figure 1. Cyclic voltammogram of **[(AA)Ni-1*][I]** in CH_3CN; all potentials referenced to NHE (* = peaks arising from iodide counterion)

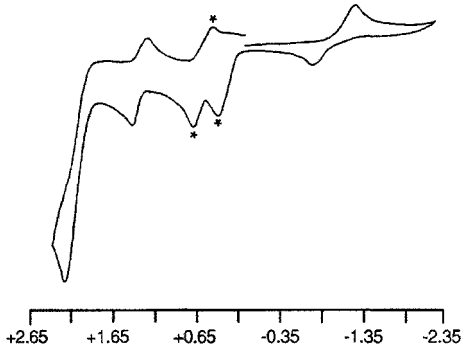

Figure 2. Cyclic voltammogram of **[$(AA)_2$Ni-1*][I_2]** in CH_3CN; all potentials referenced to NHE (* = peaks arising from iodide counterion)

Scheme 4 presents the previously well-defined redox couples of the four-coordinate methyl thioether derivatives **[(Me)Ni-1*][I]**[9] and **[$(Me)_2$Ni-1*][I_2]**[12] and the six-coordinate diacetate derivative **[$(Ac)_2$Ni-1]** for comparison to those of the acetamide complexes **[(AA)Ni-1*][I]** and **[$(AA)_2$Ni-1*][I_2]**.[15] The square planar monomethyl derivative has an $Ni^{II/I}$ redox couple ca. 750 mV more positive than that of the **Ni-1*** dithiolate precursor, while the dimethyl derivative, the dication, shows an additional positive gain of +960 mV. The enhanced accessibilities of the $Ni^{II/I}$ redox couples are attributed mainly to the positive charge resulting from successive *S*-methylations and the transformation of anionic thiolates into neutral thioether donors.[10] Consistent with this is the observation that the $Ni^{II/I}$ reduction of the neutral **[$(Ac)_2$Ni-1]** complex is not observed

when scanned to −2.0 V in CH_3CN. The increased electron density on the nickel center provided by the two anionic axial donors accounts for the negative shift.

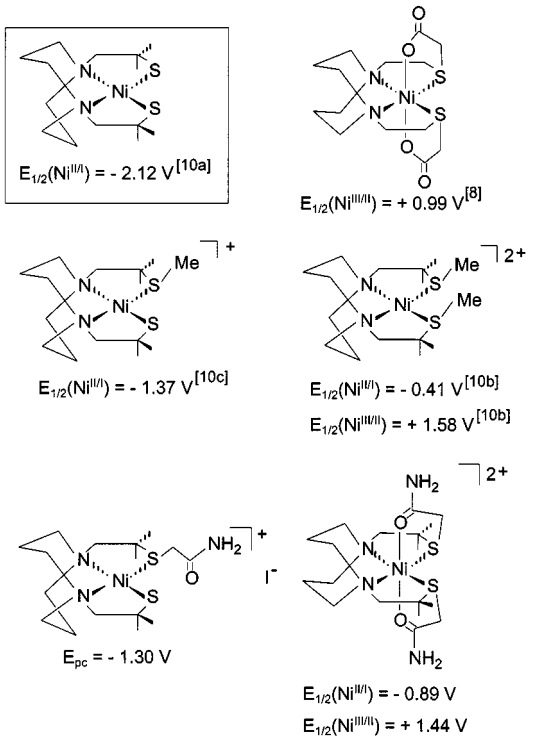

Scheme 4. Comparison of the $Ni^{II/I}$ reduction potentials ($E_{1/2}$ vs. NHE) of **[(AA)Ni-1*][I]** and **$[(AA)_2$Ni-1*$][I]_2$** with those of **[(Me)Ni-1*][I]**, **$[(Me)_2$Ni-1*$][I]_2$**, and **$[(Ac)_2$Ni-1]**

The similarity in reduction potentials of **[(AA)Ni-1*][I]** and the $Ni^{II/I}$ redox couple of **[(Me)Ni-1*][I]** suggests that the ligand environments, geometries, and charges are nearly the same in the two complexes. The dialkylated compounds differ. The increased electron density on the nickel center in the octahedral complex accounts for the relative difficulty (by ca. 480 mV) in the reduction of **$[(AA)_2$Ni-1*$][I]_2$** as compared to the four-coordinate **$[(Me)_2$Ni-1*$][I]_2$**, Scheme 4. Nevertheless, the $Ni^{II/I}$ couple of the dication is at minimum 1.1 V more positive than that of the neutral **$[(Ac)_2$Ni-1]** complex.

The anodic events for the **$[(Me)_2$Ni-1*$][I]_2$**, **$[(AA)_2$Ni-1*$][I]_2$** and **$[(Ac)_2$Ni-1]** complexes, Scheme 4, are assigned as metal-based oxidation, presumably $Ni^{II/III}$. The quasi-reversible oxidation wave for **$[(AA)_2$Ni-1*$][I]_2$** is closer in value to **$[(Me)_2$Ni-1*$][I]_2$** (ca. 140 mV more accessible) than to **$[(Ac)_2$Ni-1]** (ca. 440 mV less accessible). These results indicate that both the $Ni^{II/I}$ and the $Ni^{II/III}$ redox potentials are predominantly determined by the charge of the complex, with the addition of axial donor groups providing a lesser perturbation. The greater difference in the $E_{1/2}$ of the $Ni^{II/I}$ couples in **$[(Me)_2$Ni-1*$][I]_2$** and **$[(AA)_2$Ni-1*$][I]_2$** as compared to the difference in $E_{1/2}$ of the $Ni^{II/III}$ couples may be attributed to the following: 1) unlike the hexadentate ligand, the tetradentate N_2S_2 ligand has some capability to distort toward tetrahedral which eases the $Ni^{II/I}$ reduction; and 2) little, if any, ligand distortion is required to accommodate Ni^{3+}.

Molecular Structures

A portion of the crystal packing for **[(AA)Ni-1*][I]** is given in Figure 3 to highlight the intermolecular N···H···O interactions. Each complex cation is H-bonded to an adjacent cation via the carbonyl oxygen atoms and amide hydrogen atoms with N···O distances of 2.60(1) Å. These cations are stacked such that the pseudo six-membered cyclic structures form a channel through the lattice. The cyclic structure itself bonds externally to two iodide ions as seen in the N···I distance of 3.365(1) Å.

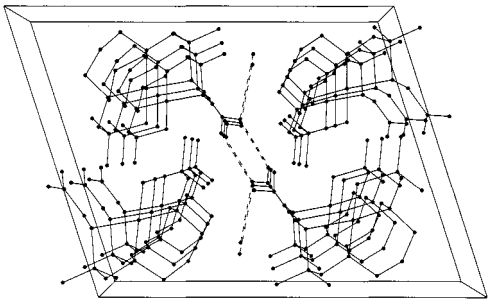

Figure 3. A portion of the crystal packing diagram of **[(AA)Ni-1*][I]** showing intermolecular hydrogen bonding; the hydrogen atoms have been omitted for clarity

Two iodide counterions and one CH_3CN solvent molecule co-crystallize with the complex cation **$[(AA)_2$Ni-1*$]^{2+}$**. The packing diagram for this salt indicates that a weak hydrogen bonding array exists between the amide hydrogen atoms and the iodide ions [I···N distances of 3.55(1) and 3.53(1) Å]; the solvent of crystallization does not appear to be involved in H-bonding.

Figures 4 and 5 display the molecular structures of the coordination complex cations of **[(AA)Ni-1*][I]** and **$[(AA)_2$Ni-1*$][I]_2$**; selected bond lengths and angles for each complex are given in Table 2. The singly alkylated compound, **[(AA)Ni-1*][I]** is four-coordinate and greatly distorted from the regular square planar geometry of the parent dithiolate complex, **Ni-1***. Despite the rigidity of the bme*-daco ligand, this distortion, a 13.6° tetrahedral twist (see Table 2 footnote), is among the largest observed for the collection of **Ni-1** and **Ni-1*** four-coordinate derivative complexes.[10−12,16] The Ni−S(2) (thioether S) distance is only slightly elongated from the Ni−S(1) (thiolate S) distance and from the average Ni−S distance [2.152(1) Å] in **Ni-1***.[11] There is no significant difference in the average Ni−N distances between **[(AA)Ni-1*][I]** and **Ni-1*** [1.995(3) Å]. Like most four-coordinate **Ni-1** and **Ni-1*** derivatives, the diazacyclooctane backbone in **[(AA)Ni-1*][I]** adopts a chair-boat configuration.

The expansion in the coordination sphere of the octahedral **$[(AA)_2$Ni-1*$][I]_2$** relative to the four-coordinate **[(Me)Ni-1*][I]** complex is seen primarily in the Ni−S dis-

Table 2. Selected bond lengths [Å], angles [°], and distortion in N_2S_2 plane [°] for **[(AA)Ni-1*][I]** and **[$(AA)_2$Ni-1*][I]$_2$**

	[(AA)Ni-1*][I]	**[$(AA)_2$Ni-1*][I]$_2$**
Ni(1)−N(1)	1.963(13)	2.100(4)
Ni(1)−N(2)	2.051(12)	2.092(4)
Ni(1)−S(1)	2.088(5)	2.402(1)
Ni(1)−S(2)	2.167(5)	2.427(1)
Ni(1)−O(1)	−	2.040(3)
Ni(1)−O(2)	−	2.052(3)
O(1)−C(16)	1.22(2)	1.238(5)
O(2)−C(18)	−	1.246(5)
C(16)−N(3)	1.330(9)	1.303(6)
C(18)−N(4)	−	1.296(6)
N(1)−Ni(1)−N(2)	89.6(5)	86.02(15)
S(1)−Ni(1)−S(2)	94.7(2)	96.44(5)
N(1)−Ni(1)−S(1)	92.3(4)	89.46(11)
N(1)−Ni(1)−S(2)	163.3(4)	172.33(12)
N(2)−Ni(1)−S(1)	175.4(4)	173.71(11)
N(2)−Ni(1)−S(2)	84.6(3)	88.45(11)
O(1)−Ni(1)−O(2)	−	167.59(13)
O(1)−C(16)−C(15)	123.3(12)	122.8(4)
O(2)−C(18)−C(17)	−	120.7(4)
N(1)−Ni(1)−O(1)	−	87.89(15)
N(1)−Ni(1)−O(2)	−	101.51(14)
N(2)−Ni(1)−O(1)	−	100.60(14)
N(2)−Ni(1)−O(2)	−	88.24(14)
S(1)−Ni(1)−O(1)	−	83.58(9)
S(1)−Ni(1)−O(2)	−	88.38(10)
S(2)−Ni(1)−O(1)	−	87.91(10)
S(2)−Ni(1)−O(2)	−	83.60(10)
N_2S_2 plane distortion[a]	13.6	6.5

[a] The N_2S_2 plane distortion angles are measured as the angle of intersection of the normals of the S(1)−X−S(2) and N(1)−X−N(2) planes, where X is the centroid of the N_2S_2 plane. As the nickel atom is not necessarily equidistant from the nitrogen and sulfur atoms, the centroid rather than Ni is used to define the planes.

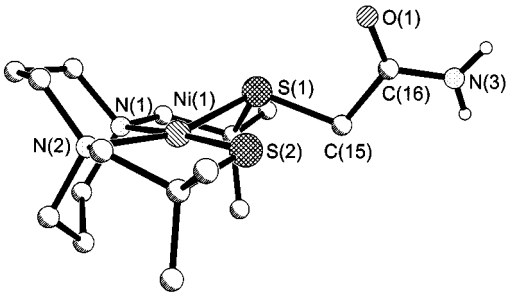

Figure 4. Ball-and-stick structure of **[(AA)Ni-1*][I]**; the iodide counterion and hydrogen atoms bonded to carbon atoms are omitted

tances (lengthened by ca. 0.3 Å). The axial atom that is bound to the nickel center also forms the shortest bond to the amide carbon atom and is thus assumed, consistent with the IR assignment above, to be O. In both **[$(AA)_2$Ni-1*][I]$_2$** and **[$(Ac)_2$Ni-1]** the diazacyclooctane framework adopts the chair-chair configuration commonly seen in other six-coordinate **Ni-1** and **Ni-1*** derivatives in which the central methylene carbon atoms are oriented towards each other and away from the $N_2S_2O_2Ni$ coordination sphere.[8,16b,17−19]

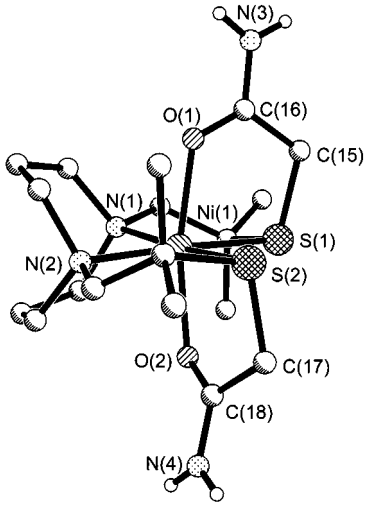

Figure 5. Ball-and-stick structure of **[$(AA)_2$Ni-1*][I]$_2$**; the iodide counterions, the solvent of crystallization and hydrogen atoms bonded to carbon atoms are omitted

Exposure to Acetylene

There are several reports of reactions of metal sulfides with acetylene to produce enedithiolates.[20] Thus, acetylene was bubbled through a CH_3CN solution of **Ni-1*** and the resultant mixture was monitored by UV/Vis spectroscopy. After 25 minutes, the spectrum of the solution was nearly identical to that of a solution containing only **Ni-1***. At that point, the addition of one equivalent of iodoacetamide caused a color change from purple to brown; the UV/Vis spectrum was found to be identical to that of **[(AA)Ni-1*][I]**. The implication is that acetylene does not inhibit or block alkylation by iodoacetamide in the Ni^{II} dithiolate complex.

Conclusion

The *cis*-dithiolates **Ni-1** and **Ni-1*** demonstrate S-nucleophilicity with iodoacetate and iodoacetamide, forming S−C bonds and at least the potential for extending the denticity of the modified N_2S_2 ligand. In all cases the thioether S-donors remain coordinated to the nickel center. Both acetamide derivatives of **Ni-1*** show positive $Ni^{II/I}$ redox couple shifts relative to the parent dithiolate, accountable mainly to increased positive charge on the complexes. In the diacetamide derivatives of **Ni-1** and **Ni-1*** the identity of the axial donor atoms as the amide oxygen atoms was suggested by X-ray crystallography and confirmed by IR spectroscopy.

Despite the excellent nucleophilicity of the *cis*-dithiolates of **Ni-1***, the presence of acetylene did not inhibit alkylation by iodoacetamide. Two possible explanations for the reported[3] protection by acetylene of the nickel-iron heterometallic site of *T. roseopersicina* [NiFe]H_2ase from iodoacetamide deactivation are as follows: 1) acetylene might serve as a molecular block which prevents iodoacetamide access to the active site; or 2) in the reduced state of the enzyme,

presumably containing Ni^{I}, acetylene might reversibly bind to the cysteine thiolates or the nickel center to prevent alkylation.

The model study above finds that terminal thiolates bound to nickel(II) are reactive with alkylating agents and maintain Ni−S(thioether) coordination. It is expected that thiolates bound to Ni^{I}, the presumed oxidation state of Ni in the reduced active form, will show similar if not enhanced reactivity. It should be noted that the structural and molecular dynamics studies[5] of the [NiFe]H_2ase enzyme were performed on coordinates derived from the oxidized, inactive form. The active, reduced form of the enzyme could have a modified access channel, one that is more accessible to larger molecules. Thus, *assuming* the iodoacetamide moiety can reach the active site Ni(S−Cys)$_2$ unit, a possible structure of the iodoacetamide-alkylated, heterobimetallic site is depicted in Scheme 5. Amide-O coordination to the nickel center forming a distorted square pyramid (not shown), could be another possible consequence of alkylation. Additionally, the open site of the d^6 iron center expected in the reduced form of the enzyme (i.e., the μ-OH group is lost)[4] could present another amide-O binding site. In any case, *S*-alkylation would disrupt the 4 to 5 Å segment which blocks access to the active site from the gas access channel. The fact that the H/D exchange reaction of H_2/D_2O is lost in the chemically modified protein is consistent with proposals that hydrogen activation takes place at the terminal Ni(S−Cys)$_2$ unit,[21] or at the open site on the iron center. On the other hand, our studies have shown that a dramatic change in redox potentials occurs upon conversion of a thiolate to a thioether by iodoacetamide alkylation. Such a redox change is expected to overwhelm the entire range of [NiFe]H_2ase activity, influencing whatever site and mechanism is operative for H_2/H^+ catalysis.

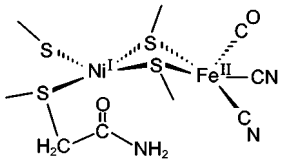

Scheme 5. One possible structural consequence of iodoacetamide alkylation at a terminal Ni(S-Cys) residue in [NiFe]H_2ase

It is noteworthy that the iodoacetamide deactivation of the zinc-metalloenzyme MetE occurs at a particular cysteine unit (Cys726), known to be bound to zinc.[2] In this case a similar chemical process of *S*-alkylation undoubtedly blocks the transfer of the methyl group from 5-methyltetrahydrofolate to homocysteine. That is, changes in redox properties are not mechanistic options.

While the Vignais study[3] suggests the possibility of active-site cysteine modification, the identity of the modified residues was not determined in the [NiFe]H_2ase examined. Histidine and carboxylate residues, reasonably good nucleophiles, are known to be somewhat reactive with alkylating agents. The modification of these and/or cysteine residues far remote from the active site could cause structural changes in the protein which might severely disrupt the active site or prevent substrate from binding. Thus, despite the clear-cut evidence offered above and elsewhere for nickel-bound thiolate reactivity, there may be factors other than active-site modification which can lead to enzyme deactivation.

Experimental Section

General Procedures: Although the products are air-stable, they are somewhat hygroscopic and should be handled using standard Schlenk or syringe techniques using N_2 (passed through a drying tube of $CaSO_4$, molecular sieves and NaOH) or an Ar-filled glovebox (Vacuum Atmospheres). Solvents were dried according to published procedures[22] and distilled under N_2. Acetonitrile was distilled once from CaH_2 and twice from P_2O_5 and freshly distilled from CaH_2 immediately before use. Reagent grade iodoacetamide (Aldrich) was used as received.

Physical Measurements: UV/Vis spectra were measured with a Hewlett-Packard 8452A diode array spectrophotometer and quartz cells of path length 1.00 cm. Infrared spectra were recorded as KBr pellets (unless otherwise specified) using an IBM IR/32 Fourier transform single-beam spectrophotometer. Elemental analyses were performed by Canadian Microanalytical Services, Delta, British Columbia, Canada. Conductance measurements were performed with an Orion Model 160 conductance meter. − Cyclic voltammograms were recorded with a BAS-100A electrochemical analyzer using $Ag^0/AgNO_3$ reference and glassy carbon working electrodes with 0.1 M tetra-*n*-butylammonium hexafluorophosphate (TBAHFP) supporting electrolyte in CH_3CN with a platinum wire auxiliary electrode. The potentials were referenced to NHE using ferrocene (+400 mV vs NHE).

Syntheses: The **Ni-1*** and **Ni-1** complexes were synthesized and purified according to published procedures.[23] Iodoacetamide was stored inside a glovebox refrigerator (−30°C) and weighed out in the glovebox immediately before use. Unless otherwise stated all reactions were performed under N_2 and at ambient temperature (22°C).

[(AA)Ni-1*][I]: Iodoacetamide (10 mg, 0.054 mmol) was dissolved in dry CH_3CN (5 mL) and transferred to a purple 5-mL acetonitrile solution containing one equivalent of **Ni-1*** (19 mg, 0.055 mmol). A color change from purple to green was immediately observed. The solution was stirred for 6 h during which time no further color change occurred. The reaction mixture was transferred via cannula to a double test tube for ether diffusion. Red brown crystals of suitable for X-ray diffraction were obtained (yield 34%). − $C_{16}H_{32}IN_3NiOS_2$ (532.18): calcd. (found) C 36.1 (36.1), H 6.06 (5.89), N 7.90 (7.85). − FT IR (KBr): ν [$^{-1}$] = 3304, 3140, 1684. − UV/Vis (MeOH): λ_{max} [nm] (ε) = 224 (20626), 264 (7967), 308 (7262), 456 (124), 604 (51).

1,5-Diazacyclooctane-1,5-diylbis(2,2-dimethyl-3-thiapentanamide)-nickel(II) Iodide {[(AA)$_2$Ni-1*][I]$_2$}: As described above, iodoacetamide (20 mg, 1.08 mmol) in 5 mL of CH_3CN was transferred to a 5-mL CH_3CN solution containing 1/2 equivalent of **Ni-1*** (19 mg, 0.055 mmol). A color change from purple to green was observed and the solution was stirred for 48 h to assure complete reaction. The green solution was transferred via cannula to a double test tube for ether diffusion. Dark blue crystals suitable for X-ray diffraction were obtained (yield 27%). − $C_{18}H_{36}I_2N_4NiO_2S_2 \cdot CH_3CN$ (758.19): calcd. (found) C 31.7 (31.7), H 5.18 (5.10), N 9.23 (9.08). − FT IR (KBr): ν [$^{-1}$] = 3236, 3100, 1645, 1591. − UV/Vis

Table 3. Crystallographic data for **[(AA)Ni-1*][I]** and **[$(AA)_2$-Ni-1*][$I]_2$**

	[(AA)Ni-1*][I]	**[$(AA)_2$Ni-1*][$I]_2$**
Emp. formula	$C_{16}H_{32}IN_3NiOS_2$	$C_{18}H_{36}I_2N_4NiO_2S_2 \cdot CH_3CN$
Mol. mass [g/mol]	532.18	758.19
Space group	monoclinic	monoclinic
	$P2_1/c$	$P2_1/c$
a [Å]	14.892(3)	19.722(4)
b [Å]	7.903(2)	8.5270(17)
c [Å]	18.896(4)	18.766(4)
β [°]	107.86(3)	112.99(3)
V [Å^3]	2116.7(7)	2905.2(10)
Z	4	4
ρ(calcd.) [g cm^{-3}]	1.670	1.733
T [K]	298(2)	293(2)
Radiation (λ [Å])	Mo-K_α (0.71073)	Mo-K_α (0.71073)
Total no. of reflns.	3874	5271
No. of obsd. reflns.[a]	3719	5095
	$I \geq 2.0\sigma I$	$I \geq 2.0\sigma(I)$
μ [$^{-1}$]	0.2581	0.2962
$R(F)$ [$I \geq 2.0\sigma(I)$][a]	6.91%	3.65%
$S(F^2)$[a]	1.153	1.042

[a] Residuals: $R(F) = \Sigma|F_o - F_c|/\Sigma F_o$; $S(F^2) = \{\Sigma w(F_o^2 - F_c^2)^2]/[N_{data} - N_{parameters}]\}^{1/2}$.

(MeOH): λ_{max} [nm] (ε) = 220 (19914), 258 (7158), 356 (29), 580 (23).

[(AA)Ni-1][I]: As described above a 10-mL CH_3CN solution of iodoacetamide (140 mg, 0.76 mmol) was transferred to a 40-mL CH_3CN solution of **Ni-1** (220 mg, 0.76 mmol). A color change from purple to dark brown was observed and the solution was stirred for 6 h. The solvent was removed in vacuo. The remaining brown solid was dissolved in dry MeOH (ca. 10 mL) and orange-brown crystals were formed from diethyl ether diffusion (yield 5.6%). − $C_{12}H_{24}IN_3NiOS_2$ (476.07): calcd. (found) C 30.3 (30.5), H 5.08 (5.05), N 8.83 (8.73). − FT IR (KBr): ν [$^{-1}$] = 3362, 3244, 3167, 1676, 1604. − UV/Vis (MeOH): λ_{max} [nm] (ε) = 224 (20048), 304 (7970), 472 (137), 592 (53).

1,5-Diazacyclooctane-1,5-diylbis(3-thiapentamide)nickel(II) Iodide {[$(AA)_2$Ni-1][$I]_2$}: Similarly, a 10-mL CH_3CN solution of iodoacetamide (195 mg, 1.05 mmol) was transferred to a solution of **Ni-1** (153 mg, 0.525 mmol) in 40 mL of CH_3CN. An immediate color change from purple to dark brown was followed by development of a blue color and then a precipitate formed over the course of 12 h. The supernatant was removed via cannula and the precipitate washed twice with dry acetonitrile (2 × 10 mL). The product was dissolved in dry MeOH (ca. 10 mL) and dark blue crystals were formed upon diethyl ether diffusion (yield 49%). − $C_{14}H_{28}I_2N_4NiO_2S_2 \cdot CH_3OH$ (693.08): calcd. (found) C 26.0 (25.8), H 4.65 (5.10), N 8.08 (8.16). − FT IR (KBr): ν [$^{-1}$] = 3240, 3125, 1649, 1590. − UV/Vis (MeOH): λ_{max} [nm] (ε) = 220 (18836), 254 (7182), 362 (51), 580 (36).

Iodoacetamide Addition to Ni-1 in the Presence of Acetylene: A 2.5-mL aliquot of a 5 mM MeCN solution of **Ni-1*** (4.3 mg, 12.5 μmol) was transferred via cannula to a UV/Vis cell. The cell was stoppered with a rubber septum and acetylene was bubbled through the solution for 25 min and the UV/Vis spectrum was recorded; it was identical to that of **Ni-1***. A 0.2-mL portion of a 62.5 mM MeCN solution of iodoacetamide (2.3 mg, 12.5 μmol) was added to the cell via syringe; the acetylene purge was resumed. After ca. 20 min, the solution color had changed from purple to brown; the acetylene bubbling was discontinued and the UV/Vis spectrum was taken. The final UV/Vis spectrum of the **Ni-1***, acetylene and iodoacetamide mixture was identical with that of isolated **[(AA)Ni-1*][I]**.

X-ray Crystallography and Structure Solution: The X-ray crystal structure analyses were carried out at the Crystal & Molecular Structure Laboratory Center for Chemical Characterization and Analysis at Texas A&M University. Crystallographic data for the complexes **[(AA)Ni-1*][I]** and **[$(AA)_2$Ni-1*][$I]_2$** are listed in Table 3; selected parameters are listed in Table 2. Preliminary examinations and data collections were performed with a Siemens P4 X-ray diffractometer. The structures were solved by direct methods [SHELXS, SHELXTL-93].[24] Both compounds crystallize in the monoclinic space group $P2_1/c$. **[(AA)Ni-1*][I]** crystallizes with two orthogonal orientations of the Ni complex relative to the iodide positions in the asymmetric unit. This produces a disordered structure. The Ni position is common to both disordered structures. The disordered portions of the Ni complex are related by a pseudo two-fold axis parallel to the a^* axis and running through the Ni atoms. Crystallographic data (excluding structure factors) for the structures reported in this paper have been deposited with the Cambridge Crystallographic Data Center as supplementary publication nos. CCDC-102633 and -102634. Copies of the data can be obtained free of charge on application to CCDC, 12 Union Road, Cambridge CB2 1EZ, UK [Fax: int. code + 44-1223/336-033; E-mail: deposit@ccdc.cam.ac.uk].

Acknowledgments

Financial support from the National Science Foundation (CHE 94−15901) with contributions from the R. A. Welch Foundation for the work and NSF-CHE 85−13273 for the X-ray diffractometer and crystallographic computing system are gratefully acknowledged.

[1] R. L. Lundblad, *Chemical Reagents for Protein Modification*, 2nd ed., CRC Press, Boca Raton, Florida, **1991**, pp. 59−93.
[2] [2a] J. C. Gonzalez, R. V. Banerjee, S. Huang, J. S. Sumner, R. G. Matthews, *Biochemistry* **1992**, *31*, 6045. − [2b] J. C. Gonzalez, K. Peariso, J. E. Penner-Hahn, R. G. Matthews, *Biochemistry* **1996**, *35*, 12228.
[3] N. A. Zorin, B. Dimon, J. Gagnon, J. Gaillard, P. Carrier, P. M. Vignais, *Eur. J. Biochem*. **1996**, *241*, 675.
[4] [4a] A. Volbeda, M.-H. Charon, C. Piras, E. C. Hatchikian, M. Frey, J. C. Fontecilla-Camps, *Nature* **1995**, *373*, 580. − [4b] A. Volbeda, E. Garcin, C. Piras, A. L. de Lacey, V. M. Fernandez, E. C. Hatchikian, M. Frey, J. C. Fontecilla-Camps, *J. Am. Chem. Soc*. **1996**, *118*, 12989. − [4c] A. L. de Lacey, E. C. Hatchikian, A. Volbeda, M. Frey, J. C. Fontecilla-Camps, V. M. Fernandez, *J. Am. Chem. Soc*. **1997**, *119*, 7181. − [4d] M. Frey, *Struct. Bonding* **1998**, *9*, 97, and references therein. − [4e] J. C. Fontecilla-Camps, *J. Biol. Inorg. Chem.* **1996**, *1*, 91, and references therein.
[5] Y. Montet, P. Amara, A. Volbeda, X. Vernede, E. C. Hatchikian, M. J. Field, M. Frey, J. C. Fontecilla-Camps, *Nat. Struct. Biol*. **1997**, *4*, 523.
[6] [6a] R. Cammack, C. Bagyinka, K. L. Kovacs, *Eur J. Biochem*. **1989**, *182*, 357. − [6b] S. P. J. Albracht, *Biochim. Biophys. Acta* **1994**, *1188*, 167.
[7] R. P. Happe, W. Roseboom, A. J. Plerik, S. P. J. Albracht, K. A. Bagley, *Nature* **1997**, *385*, 126. K. A. Bagley, E. C. Duin, W. Roseboom, S. P. J. Albracht, W. H. Woodruff, *Biochemistry* **1995**, *34*, 5527.
[8] D. C. Goodman, T. Tuntulani, P. J. Farmer, M. Y. Darensbourg, J. H. Reibenspies, *Angew. Chem. Int. Ed. Engl.* **1993**, *32*, 116.
[9] This complex has been previously characterized by X-ray crystallography. A more detailed report of its properties will be presented in another paper.

[10] P. J. Farmer, J. H. Reibenspies, P. A. Lindahl, M. Y. Darensbourg, *J. Am. Chem. Soc*. **1993**, *115*, 4665.
[11] M. Y. Darensbourg, I. Font, M. Pala, J. H. Reibenspies, *J. Coord. Chem*. **1994**, *32*, 39.
[12] G. Musie, J. H. Reibenspies, M. Y. Darensbourg, *Inorg. Chem*. **1998**, *37*, 302.
[13] W. J. Geary, *Coord Chem Rev.* **1971**, *7*, 81.
[14] [14a] L. A. Scheich, P. Gosling, S. J. Brown, M. M. Olmstead, P. K. Mascharak, *Inorg. Chem*. **1991**, *20*, 1677. – [14b] H. C. Freeman, N. D. Hutchinson, *Acta Crystallogr., Sect. B.* **1979**, *35*, 2045. – [14c] D. Fenske, N. Mronga, K. Dehnicke, *Z. Anorg. Allg. Chem*. **1981**, *482*, 106. – [14d] J.-L. Du, S. J. Rettig, R. C. Thompson, J. Trotter, P. Betz, A. Bino, *Can. J. Chem*. **1992**, *70*, 732. – [14e] M. S. Konigs, W. C. Dow, D. B. Love, K. N. Raymond, S. C. Quay, S. M. Rocklage, *Inorg. Chem*. **1990**, *29*, 1488. – [14f] D. J. McCabe, E. N. Dueslar, R. T. Paine, *Inorg. Chem*. **1988**, *27*, 1220.
[15] While the diacetate derivative of **Ni-1*** has not been isolated in significant yield, its spectroscopic properties are very similar to those of **[(Ác)$_2$Ni-1]**.
[16] [16a] D. K. Mills, J. H. Reibenspies, M. Y. Darensbourg, *Inorg. Chem*. **1990**, *29*, 4364. – [16b] D. C. Goodman, R. M. Buonomo, P. J. Farmer, J. H. Reibenspies, M. Y. Darensbourg, *Inorg Chem*. **1996**, *35*, 4029. – [16c] R. M. Buonomo, I. Font, M. J. Maguire, J. H. Reibenspies, T. Tuntulani, M. Y. Darensbourg, *J. Am. Chem. Soc*. **1995**, *117*, 963.
[17] D. C. Goodman, P. J. Farmer, M. Y. Darensbourg, J. H. Reibenspies, *Inorg. Chem.* **1996**, *35*, 4989.
[18] R. M. Buonomo, J. H. Reibenspies, M. Y. Darensbourg, *Chem. Ber*. **1996**, *129*, 779.
[19] D. C. Goodman, J. H. Reibenspies, N. Goswami, S. Jurrison, M. Y. Darensbourg, *J. Am. Chem. Soc*. **1997**, *119*, 4955.
[20] M. Rakowski DuBois, B. R. Jagirdar, S. Dietz, B. C. Noll, *Organometallics* **1997**, *16*, 294, and references therein.
[21] L. M. Roberts, P. A. Lindahl, *Biochemistry* **1994**, *33*, 14339.
[22] A. J. Gordon, R. A. Ford, *The Chemist's Companion*, Wiley and Sons, New York, **1972**, pp. 429–436.
[23] D. K. Mills, I. Font, P. J. Farmer, Y.-M. Hsiao, T. Tuntulani, R. B. Buonomo, D. C. Goodman, G. Musie, C. A. Grapperhaus, M. J. Maguire, C.-H. Lai, M. L. Hatley, J. J. Smee, J. A. Bellefeuille, M. Y. Darensbourg, *Inorg. Synth.* **1998**, *32*, 89.
[24] [24a] G. M. Sheldrick, *SHELXS-86*, Institut für Anorganische Chemie der Universitat, Göttingen, Germany, **1986**. – [24b] G. M. Sheldrick, *SHELXL-93*, Institut für Anorganische Chemie der Universitat, Göttingen, Germany, **1993**.

Received August 19, 1998
[I98281]